JACS
JOURNAL OF THE AMERICAN CHEMICAL SOCIETY

Article

pubs.acs.org/JACS

Protein-Triggered Supramolecular Disassembly: Insights Based on Variations in Ligand Location in Amphiphilic Dendrons

Diego Amado Torres,[†] Matteo Garzoni,[§] Ayyagari V. Subrahmanyam,[†] Giovanni M. Pavan,*[,§] and S. Thayumanavan*[,†]

[†]Department of Chemistry, University of Massachusetts, Amherst, Massachusetts 01003, United States

[§]Department of Innovative Technologies, University of Applied Science of Southern Switzerland, Manno 6928, Switzerland

Supporting Information

ABSTRACT: We use monodisperse dendrons that allow control over functional group presentation to investigate the influence of the location of a ligand on protein-induced disassembly and release of encapsulated small molecules. Based on both experiments and molecular dynamics simulations, we demonstrate that ligand location greatly influences release of guest molecules from the dendron-based supramolecular assembly. We show that a ligand moiety grafted to the dendron periphery is more accessible for the target protein in aqueous solution. On the other hand, the ligand moiety placed at the focal point or at the intermediate layer within the dendritic scaffold is less accessible, since it is surrounded by an environment rich in PEG chains, which hinders binding and even influences nonspecific interactions. We also demonstrate that the specific binding between one ligand and the target protein can destabilize the dendritic assembly. Furthermore, if more ligands are available, multivalent interactions are also possible with extravidin, which speed up disassembly and trigger the release of hydrophobic guests.

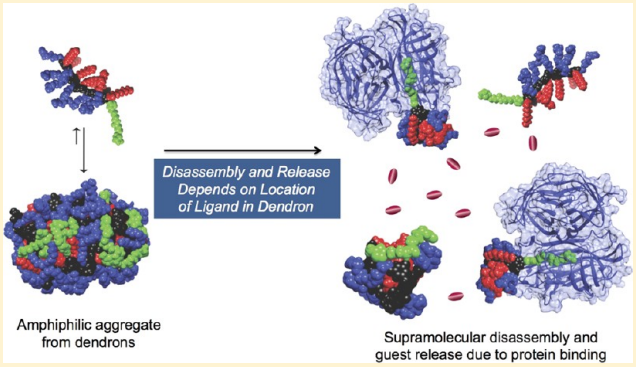

INTRODUCTION

Host systems that can spontaneously self-assemble and stably encapsulate guest molecules under one set of conditions, but disassemble and release the guest molecules when external conditions change, have been of great interest in supramolecular chemistry due to implications in a variety of biomedical applications.[1] While earlier studies have primarily focused on the former (i.e., self-assembly and binding), there has been a recent surge in interest in the latter features (disassembly and release in response to an environmental change). Also, the responsiveness of the assemblies has primarily focused on physical or chemical changes. For example, there has been a significant interest in systems that disassemble in response to chemical stimuli such as pH[2] or redox[3] variation as well as physical stimuli such as light,[4] temperature,[5] or a magnetic field.[6] While systems incorporating features sensitive to light and magnetic field have been designed to respond to external triggers for biological applications, pH- and redox-responsive systems have been designed to respond to the inherent imbalances observed in certain disease tissues. The anomalous pH or redox conditions in disease locations can be considered to be secondary imbalances in biology, as the primary imbalances are often the result of aberrant protein concentrations or enzymatic activity.[7] Therefore, there is a growing interest in developing supramolecular systems that respond to these primary factors in biology.[8]

Protein-responsive systems can be broadly classified into two categories, *viz.* covalent modification of the hosts to disable their capacity to hold the guest molecules and noncovalent binding to the host assemblies to produce the same effect.[9,10] The former is often achieved by an enzyme-driven chemical reaction that modulates the host characteristics of the molecule. In the latter case, this is achieved due to a noncovalent binding interaction. While there have been several systems designed to be degraded or covalently modified by enzymes,[10] supramolecular assemblies that lose their host capacities due to noncovalent binding with proteins have been limited. Among the systems that undergo binding-induced disassembly, polyelectrolyte assemblies that can noncovalently bind a complementarily charged surface to cause a disassembly have attracted some attention.[11] Although nonspecific in its interaction, the simplicity of these systems has proved useful in applications such as separations.[12] It has also been clear that for a binding-induced approach to be useful in applications such as delivery and sensing, where specificity is critical, strategies that use specific ligand−protein interactions are needed.[13] Since dendritic macromolecules can be produced in high molecular weights, but with a great degree of control, these scaffolds have certain unique advantages for this strategy.[14] For example, the critical aggregate concentrations (CAC) of the dendrimer-

Received: January 20, 2014
Published: March 18, 2014

   dx.doi.org/10.1021/ja500634u | *J. Am. Chem. Soc.* 2014, 136, 5385−5399

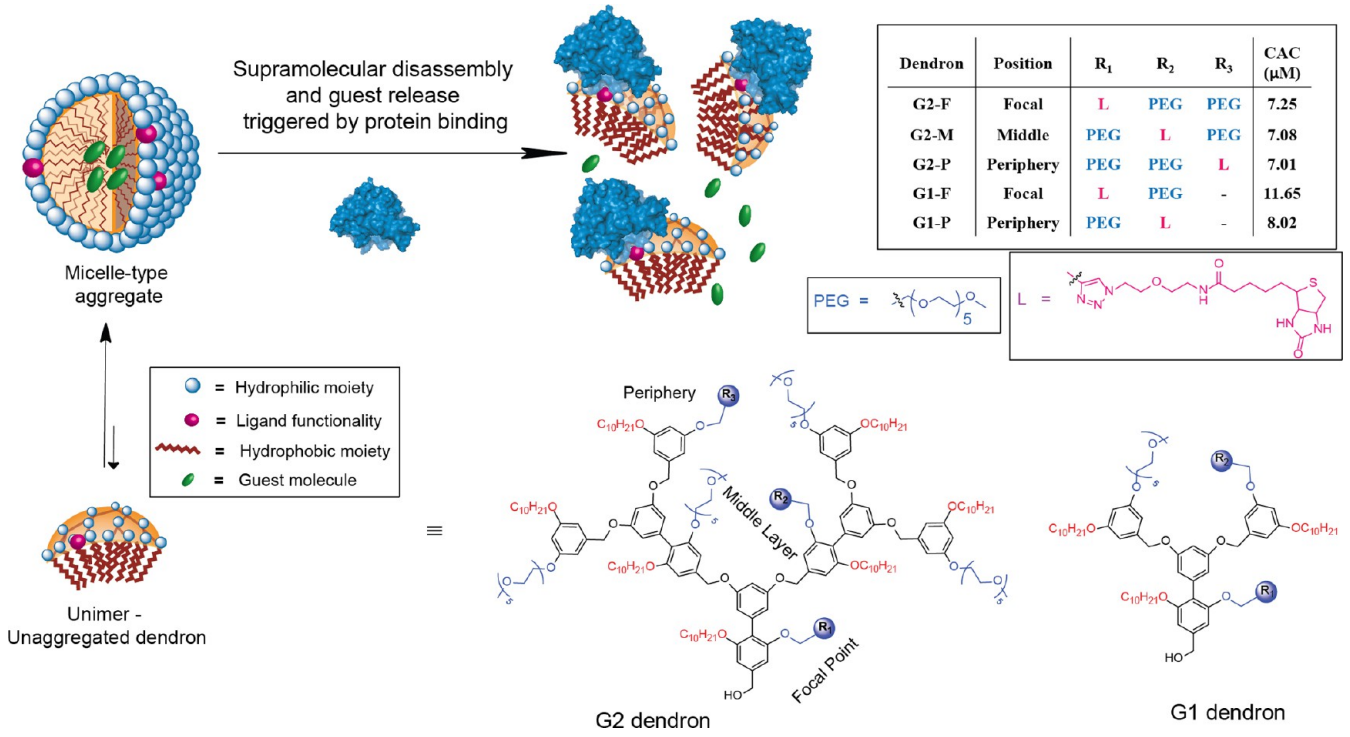

Dendron	Position	R_1	R_2	R_3	CAC (μM)
G2-F	Focal	L	PEG	PEG	7.25
G2-M	Middle	PEG	L	PEG	7.08
G2-P	Periphery	PEG	PEG	L	7.01
G1-F	Focal	L	PEG	-	11.65
G1-P	Periphery	PEG	L	-	8.02

Figure 1. Structure of the G1 and G2 containing ligands at specific locations. The CAC of each of these dendrons are listed in the table. The scheme is an illustration of the self-assembling dendrons with sequestered hydrophobic guest molecules, which are released in response to protein binding. The equilibrium illustrated in the illustration is to indicate the possible unimer-aggregate equilibrium.

based amphiphilic assemblies are low, an advantage that polymeric systems have over small molecule-based amphiphilic assemblies. Similarly, the control over functional group placements in dendritic architectures captures the advantage that small molecules have over their polymeric counterparts.[15] These features allow for structure–property relationship studies that unravel the factors that underlie the binding-induced supramolecular disassembly process. In this manuscript, we take advantage of this unique feature by incorporating ligands at specific locations within facially amphiphilic dendrons and interrogating the efficiency of the supramolecular disassembly and molecular release in response to a specific protein binding event. We use both experiments and molecular dynamics (MD) simulations synergistically to gain insights into the ligand–protein recognition-based disassembly event.

RESULTS AND DISCUSSION

Molecular Design and Synthesis. Facially amphiphilic dendrons, containing a biaryl-based internal repeat unit and an aryl peripheral unit, bear both hydrophilic and hydrophobic functional groups as side chains in each of these repeat units.[16] The amphiphilic functional groups are placed at opposite faces of the biaryl backbone of the dendron such that these molecules are endowed with the capability to form micelle-like assemblies in aqueous solution and form inverse micelle-like assemblies in apolar solvents.[17] In our preliminary findings, we have shown that placing a ligand moiety at the hydrophilic face of the dendron can provide binding-induced disassembly of the micelle-like structure in the aqueous solvent.[13a] In that work, the ligand moiety was placed at the focal point of the dendron, as this structure is synthetically most easily accessible. However, the release efficiency of guests, following protein binding, was relatively moderate. In order to fully realize the potential of this process, it is critical that we understand the effect of the functional group placement, thus taking advantage of one of the most prominent features of dendritic architectures in this supramolecular process. Therefore, in this manuscript, we investigate the effect of the placement of a protein-specific ligand moiety at specific positions of a dendron upon the accessibility of the complementary protein to the supramolecular assembly and hence the effects on the concomitant guest release response (Figure 1). The relative encapsulation of functional groups, when placed in the periphery vs the focal point of the dendron is well-known.[18] Note however that the facially amphiphilic dendrons, utilized here, have two distinct characteristics in this context: (i) the ligand moieties placed in the hydrophilic face of the dendron is attached through a rather long ethyleneglycol linker. Therefore, the classical encapsulation by the dendritic backbone should not apply here; (ii) it has been previously shown using carboxylic acid based facially amphiphilic dendrimers that these functional groups are available for nonspecific binding to the positively charged surface of chymotrypsin.[12f] For these reasons, it is important that we investigate the effect of ligand placement on the binding-induced release.

The CAC of even the first generation of these dendrons is substantially lower than the corresponding amphiphilic small molecule (μM compared to mM). Note that this 3 orders of magnitude difference in CAC is not accounted for by the simple difference in molecular weight of the amphiphilic molecules. Within each generation of dendrons however, the CAC gain has been relatively small, if any, especially when one accounts for the difference in molecular weights. Therefore, we focused on the G1 and G2 dendrons, which provide sufficient variations in the functional group placement. We targeted five different dendrons within these two generations, where the

dx.doi.org/10.1021/ja500634u | J. Am. Chem. Soc. 2014, 136, 5385–5399

Scheme 1. Synthesis of G1-P, Installment of Ligand at the Periphery

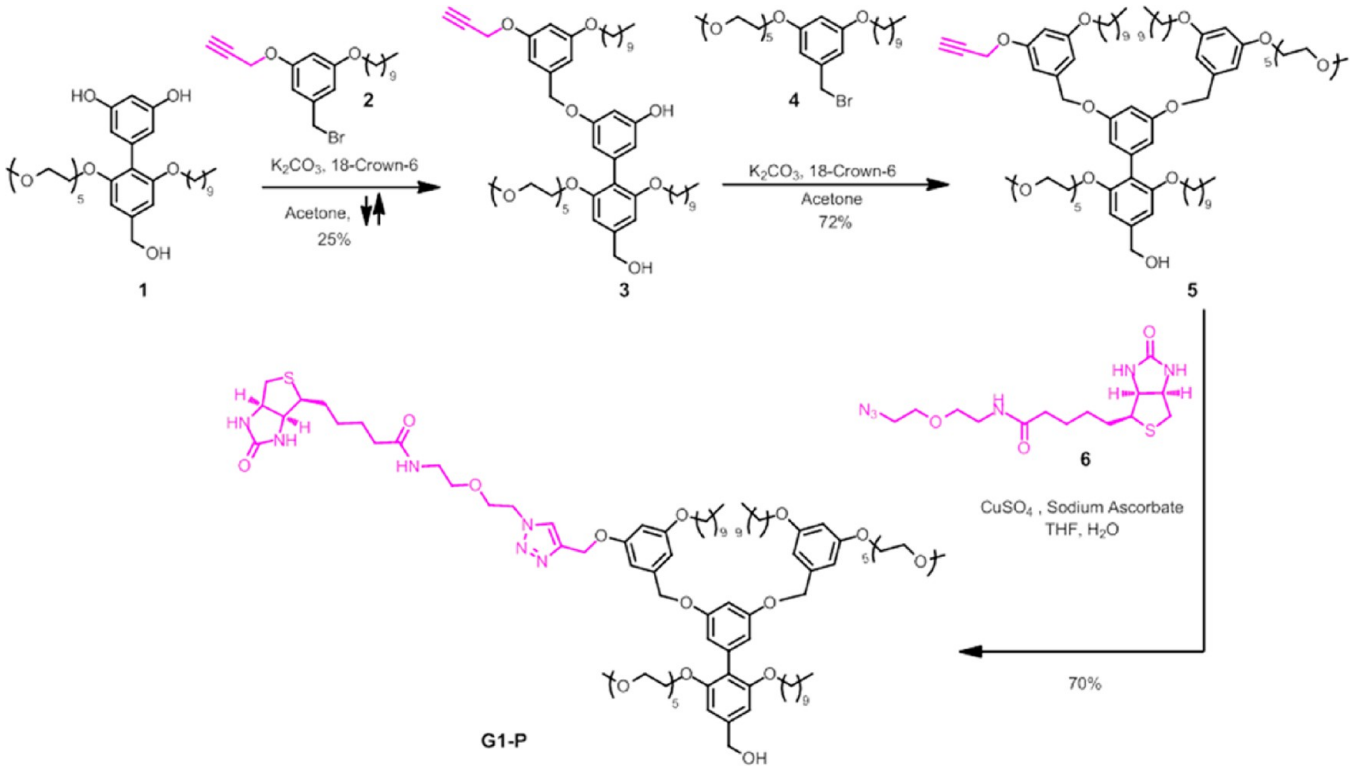

ligand placement is the key difference (see Figure 1 for the structures). Pentaethyleneglycol monomethyl ether (PEG) was chosen as the hydrophilic moiety not only for its ability to provide the requisite solubility in the aqueous phase but also for its propensity to present a charge neutral surface on the assembly that exhibits minimal nonspecific interactions.[19] Decyl moieties were incorporated as the hydrophobic components of the amphiphile. Biotin was chosen as the ligand, because of its well-established high affinity toward avidin.[20]

A ligand can be incorporated on a G1 dendron either at the focal point or at the periphery. On a G2 dendron, a ligand can be incorporated on three different layers: (i) the focal point; (ii) the middle layer; and (iii) the periphery. To install a single ligand at a specific place, one of the PEG units was replaced by the ligand, attaching it to the dendron backbone via a hydrophilic linker. This placement allows the ligand to be exposed to the aqueous solution on the hydrophilic face of the assembly. Note that the focal point is synthetically the easiest place to attach a single functional group, since the focal point is a single and unique position in a dendron. In contrast, to install a single functional group at the periphery, one has to distinguish one of the peripheral monomers from otherwise identical ones within the dendron. The G1 dendron has two such identical positions in the periphery, while the G2 dendron has four such locations. Similarly, the middle layer of the G2 dendron contains two similar positions that need to be distinguished for specifically placing a ligand moiety. Accordingly, the degree of difficulty in placing a unique functional group in the dendron increases as we move from the focal point to the periphery and as we increase the generation. To achieve these selective functionalization, we and others have developed a variety of synthetic strategies that afford multifunctionalized dendrons and dendrimers.[15,21] In all our syntheses, we initially targeted dendrons containing an acetylene moiety, which will be used as the handle to 'click' the biotin moiety in the last steps of the syntheses. Overall, we made the syntheses of the dendrons modular in order to assemble the targeted dendrons in small number of steps. Accordingly, we first synthesized the biaryl, amphiphilic AB_2 monomer **1**, the propargyl-functionalized periphery unit **2**, and the nonfunctionalized amphiphilic periphery unit **4** following the previously reported procedures.[13a] To achieve the targeted dendron **5**, the biaryl monomer **1** was first monoalkylated with a periphery unit **2** to get the propargyl-functionalized scaffold **3** (Scheme 1) in 25% yield. The low isolated yield was because of the statistical distribution of mono- and disubstituted products obtained in this reaction. Molecule **3** was then treated with the amphiphilic peripheral monomer **4** under similar alkylation conditions to achieve the G1 dendron **5** containing the reactive propargyl moiety at its periphery. The G1 dendron **5** was then treated with the azide-modified biotin **6** under alkyne−azide click chemistry conditions[22] in the presence of cupric sulfate and sodium ascorbate to obtain **G1-P** in 70% yield. Similarly, the molecule **G1-F** was prepared by clicking the biotin azide to the propargyl moiety present in the biaryl repeat unit (see Supporting Information for synthetic details).

The syntheses of the targeted G2 dendrons were achieved using a similar set of synthetic strategies, as shown in Scheme 2. To achieve the syntheses of these dendrons, the previously reported[13a] amphiphilic G1 dendron **7** was treated with the biaryl monomer **1**, where the monoalkylated product **8** was separated from a statistical mixture in 24% yield. This molecule was then treated with the bromomethyl dendron **9** (obtained from the precursor to **G1-F** in one step) or **10** (obtained from **5** in one step) to obtain the G2 dendrons **11** or **12**, containing the propargyl moiety at the middle layer or the periphery of the dendron, respectively. Copper-catalyzed Huisgen reaction of **11** and **12** with the azide-functionalized ligand **6** afforded the **G2-**

dx.doi.org/10.1021/ja500634u | J. Am. Chem. Soc. 2014, 136, 5385−5399

Scheme 2. Synthesis of G2-M and G2-P

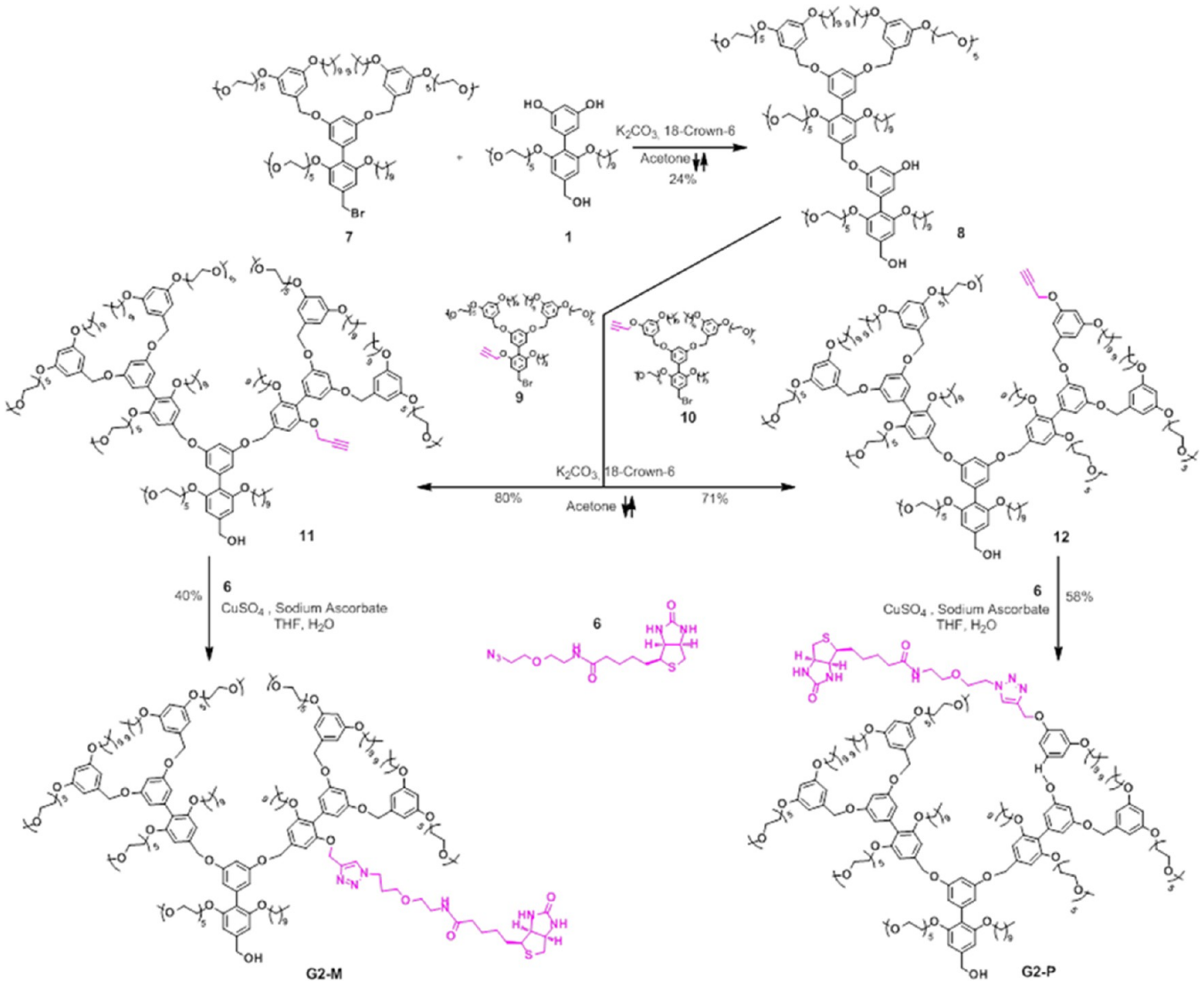

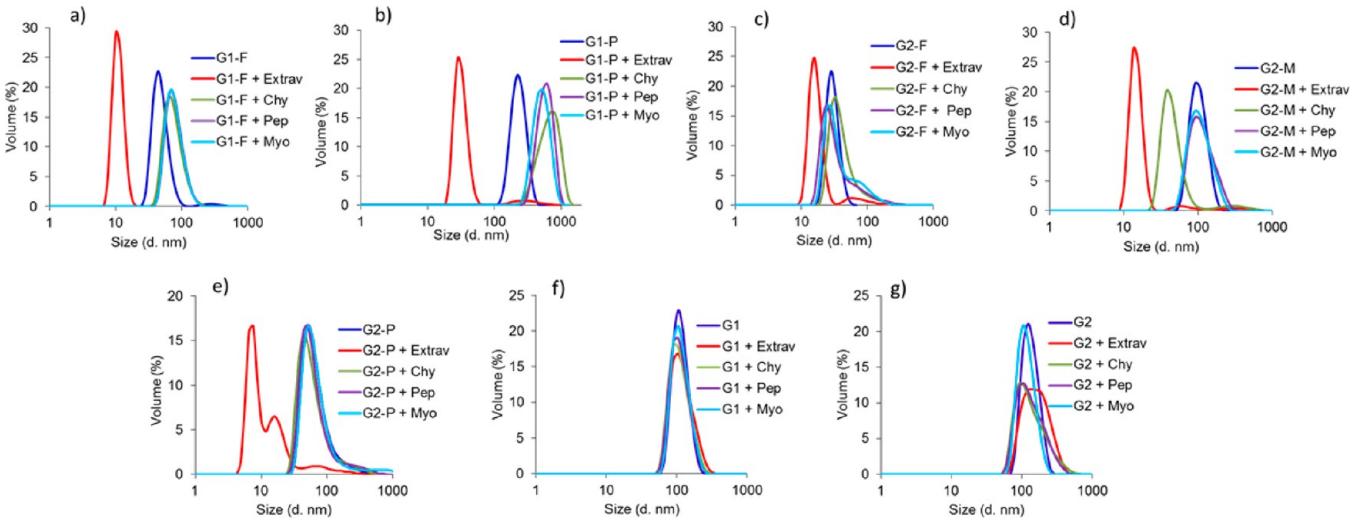

Figure 2. DLS-based measure of size change of dendritic assemblies in aqueous phase upon interaction with different proteins. (a) **G1-F**, (b) **G1-P**, (c) **G2-F**, (d) **G2-M**, (e) **G2-P**, and (f) G1 and (g) G2 control dendrons.

dx.doi.org/10.1021/ja500634u | *J. Am. Chem. Soc.* 2014, 136, 5385−5399

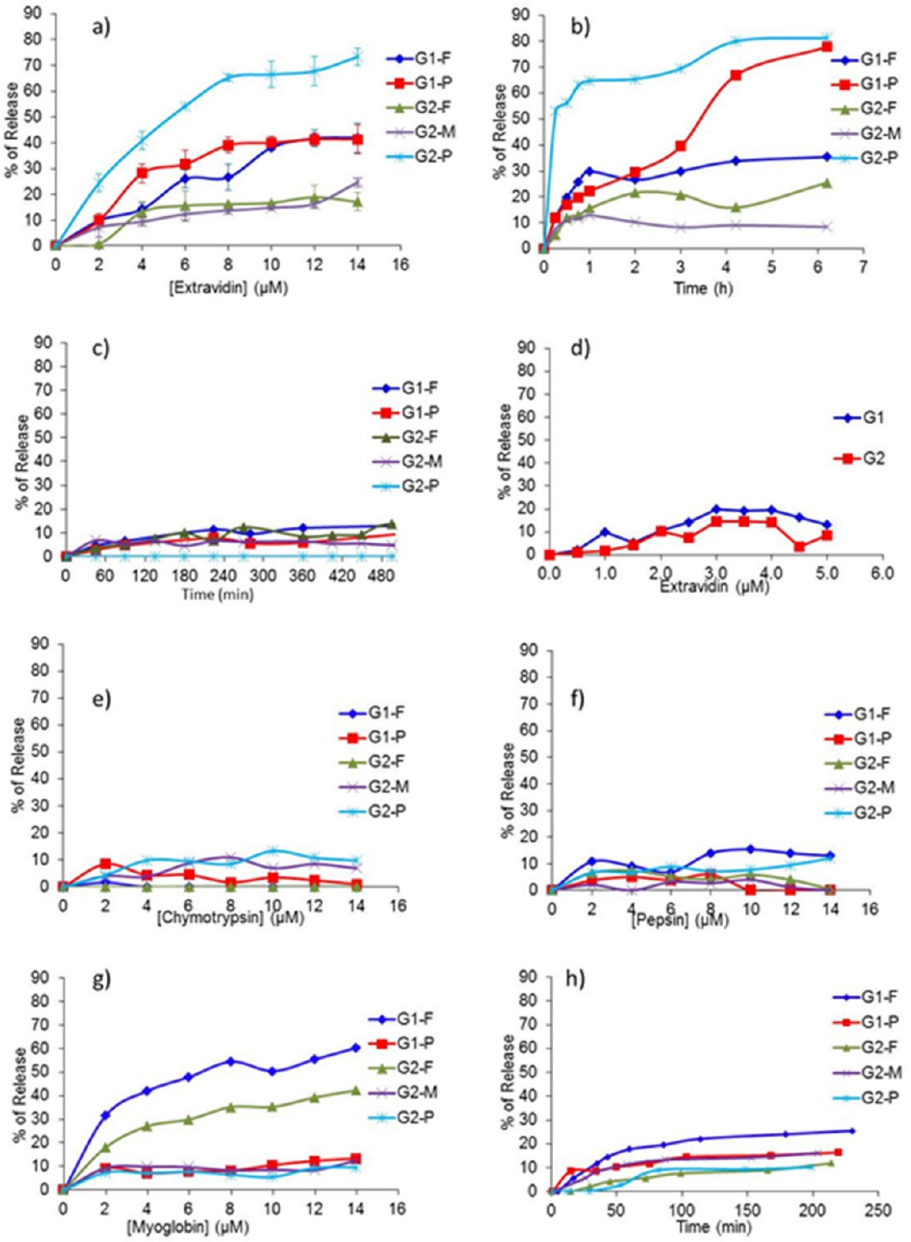

Figure 3. Fluorescence-based percentage of release of guest molecules from the amphiphilic dendritic assemblies: (a) with increasing concentration of extravidin, (b) time-dependent release in the presence of 14 μM of extravidin, (c) in buffer solutionin the absence of proteins, (d) in assemblies based on control dendrons when exposed to extravidin, (e) with increasing concentration of Chy, (f) with increasing concentration of Pep, (g) with increasing concentration of Myo. (h) Absorption-based percentage of release upon interaction of dendrons with 14 μM of Myo.

M and **G2-P** dendrons, respectively. As with **G1-F**, the **G2-F** dendron was obtained by clicking the biotin azide to the propargyl moiety present in the biaryl repeat unit (see Supporting Information for synthetic details).

Assembly and Disassembly. First, the self-assembly properties of these dendrons were studied by measuring their CACs using Nile red as the hydrophobic, spectroscopic probe (Figure S1). As anticipated, the CACs of final G1 and G2 dendrons were determined to be in the low micromolar range with values of 11.65 and 8.02 μM for **G1-F** and **G1-P**, respectively; 7.25, 7.08, and 7.01 μM for **G2-F**, **G2-M**, and **G2-P**, respectively. With the installment of a single ligand at different layers of a dendron and after knowing the lowest concentration at which they assemble into nanostructures, we investigated the response of the different dendritic aggregates in presence of the complementary protein extravidin and in presence of noncomplementary proteins with diverse pI values and molecular weights, *viz*. α-chymotrypsin (Chy, pI = 8.1–8.6), pepsin (Pep, pI = 2.9), and myoglobin (Myo, pI = 7.2), as shown in Figure 2.

Prior to analyzing the interaction between the dendritic assemblies and the proteins, we analyzed the size of the assemblies in aqueous phase using dynamic light scattering (DLS), with G1 dendron concentrations of 12.5 μM and G2 dendron concentrations of 10 μM (both above their respective CACs). The sizes of the assemblies were found to be in a few tens of nanometers, ranging from ∼30 to ∼200 nm, 44 nm for **G1-F**, 220 nm for **G1-P**, 29 nm for **G2-F**, 92 nm for **G2-M**, and 51 nm for **G2-P**. The reason for the variations in size with the subtle change in the position of the ligand is not clear.

dx.doi.org/10.1021/ja500634u | *J. Am. Chem. Soc.* 2014, 136, 5385–5399

However, note that the replacement of a hydrophilic PEG chain in a G1 or G2 dendron by a less hydrophilic pendant biotin decreases the PEG density on the assembly surface, decreasing hydrophilicity and increasing the chance of nonspecific interactions with noncomplementary proteins. Such decrease in PEG density could be more relevant in G1, where substituting one of the three PEG chains in a dendron molecule could mean a reduction of up to 33%, while such a reduction in G2 is about 14%. It is possible that these differences confer changes in the way the assemblies pack together in solution, which results in size variations among the biotin-functionalized dendrimeric assemblies.

It is interesting that the size of all these assemblies reduced to about ∼13 nm in presence of the protein, extravidin (2 μM) (Figure 2). A particular difference in disassembly among the biotin-functionalized dendrons was observed in the case of the **G2-P** that disassembled into smaller aggregates (∼7−8 nm) in presence of extravidin (Figure 2e). **G1-P** also presented some deviations, showing larger aggregates (∼28 nm) that could be formed by further aggregation of smaller protein−dendron complexes.

The decrease in the size of the assemblies was observed only in presence of the complementary protein, extravidin. In the presence of the noncomplementary proteins, no size decrease was observed, although a tendency of the biotin-functionalized dendrimeric assemblies to increase in size, forming larger aggregates, was noticed for **G1-F** and **G1-P** (Figure 2a,b). This aggregate enlargement did not occur when control dendrons with PEG replacing the ligand moiety were exposed to the same proteins, even after 15 h (Figure 2f,g). This suggested that the higher density of biotin functionalization in the G1 dendrons is the likely reason for such aggregate enlargement.

Release of Encapsulated Guest Molecules. Next, we investigated the host capabilities of the dendrons in the presence and absence of complementary and noncomplementary proteins. Specifically, we were interested in assessing the effect of incorporating the ligand moieties at different locations within the dendrons upon the disassembly-induced guest release from the dendrimer host. To investigate these differences, Nile red was encapsulated in the micelle-like nanoassemblies, and its release was triggered as a consequence of binding-induced disassembly upon exposure to extravidin. Nile red is a hydrophobic molecule that exhibits reduced fluorescence in water, unless it is sequestered in a hydrophobic pocket. Therefore, the reduction in fluorescence is a good indicator of the binding-induced disassembly event.

As shown in Figures 3a,b, small differences in placement of the ligand in the dendron produced rather different responses. First, percentage of released dye was assessed after exposing 25 μM solutions of the dendrons to increasing concentrations of extravidin. We noticed that **G1-P** and **G2-P** responded to increasing concentrations of extravidin more than other dendrons studied. To further evaluate this behavior, we monitored the release profiles over time for all the dendritic assemblies upon exposing these assemblies to 14 μM extravidin (Figure 3b). In the first hour, the release in the **G2-P** assembly was as high as 65%, while that of the **G1-P** assembly was around 22% increasing to 40% after 3 h. Interestingly, the release from the **G1-P** assembly ultimately reached about 77%, which is comparable with the 81% observed for **G2-P**. In comparison, similar exposures to extravidin resulted in 35%, 25%, and 13% for **G1-F**, **G2-F**, and **G2-M**, respectively. The extent of release observed for **G1-F** and **G2-F** is consistent with our prior observation.[13a] Interestingly, the release from **G2-M** aggregates is comparable to the release percentages observed due to nonspecific interactions.

As a control experiment, the release of the Nile red from the dendritic assemblies was also monitored in the absence of any protein (Figure 3c). No discernible release (<10%) was seen in these dendritic assemblies. Similarly, control dendrons that lack the biotin ligand also did not exhibit appreciable dye release in the presence of extravidin (Figure 3d). These results show that the release profiles observed in Figure 3a,b are indeed due to the ligand−protein binding. Moreover, it is clear that among the second generation dendrons, **G2-P** assembly is the only one that releases the hydrophobic guests efficiently following the extravidin binding.

To further test the selectivity in the systems toward the target protein, the biotin-functionalized dendrons were exposed to increasing concentrations of noncomplementary proteins, Chy, Pep, and Myo monitoring the change in Nile red fluorescence (Figure 3e−g). No significant change in the emission intensity was observed for any of the dendrons in the presence of Chy and Pep. However, while Myo did not exhibit any change in the fluorescence intensity in the **G1-P**, **G2-M**, and **G2-P** based assemblies, there was a significant change in fluorescence in the **G1-F** and **G2-F** based assemblies (Figure 3g and S3). Interestingly, these latter dendrons also exhibited much smaller release in response to extravidin (Figure 3b). It is noteworthy that Myo is a metalloprotein, and therefore the cofactors in metalloproteins could be simply quenching the fluorescence of the dye molecule without the need for releasing the contents from the amphiphilic assembly. In fact, such a phenomenon has been previously observed with polymer−surfactant coassemblies.[11c]

To test this possibility, we investigated the percentage of Nile red release in the presence of Myo by absorption spectroscopy. If it is simply a quenching phenomenon, there should be no change in the absorption spectrum since all dye molecules are still confined in the amphiphilic assembly without being released. Indeed, we noted that there was no change in the absorption spectrum over time, which suggested that the observed increase in release percentage, i.e., decrease in Nile red fluorescence, is likely due to quenching (Figure 3h).

As a second step, we were interested in gaining insights into the mechanism for the observed fluorescence reduction in the presence of Myo, especially for **G1-F** and **G2-F**. Two limiting mechanisms are possible: (i) inherently different encapsulation stabilities among the dendritic assemblies, causing the dye to leak out of **G1-F** (or **G2-F**) and to move to the hydrophobic pockets in Myo, where the proximity between the metalloprotein cofactor and the dye molecule causes fluorescence quenching; or (ii) nonspecific interactions between assemblies formed by **G1-F** (or **G2-F**) and Myo to bring the encapsulated dye molecules in proximity to the metalloprotein cofactor favoring quenching.

The mechanism (i) implies leakage of the cargo and "re-encapsulation" in the metalloprotein pockets. To test this possibility, we used a recently reported polymeric nanogel that has been well-established to have cross-link density-dependent encapsulation stabilities.[23] Nile red-encapsulated nanogels with 0%, 20%, and 50% cross-link densities were exposed to Myo. If mechanism (i) was possible, there should be a cross-link density-dependent leakage based quenching. In all cases, we found that the extent of quenching was quite independent of the cross-link density (Figure S4a,b). The quenching however

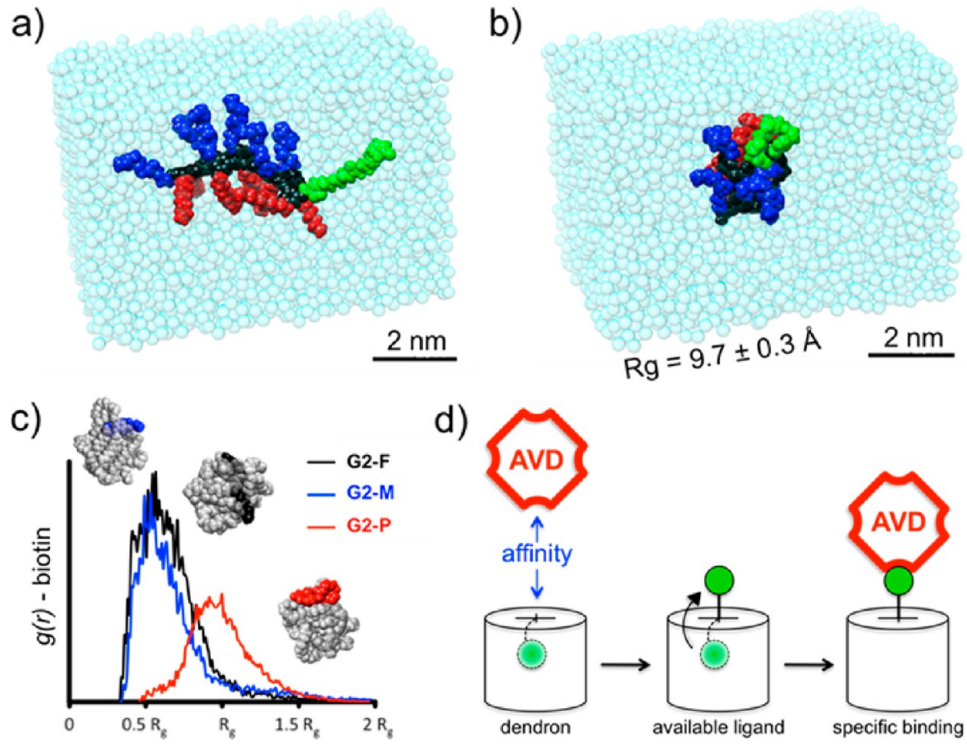

Figure 4. MD simulation of G2 dendrons in water. (a) Starting configuration of **G2-P** immerged in a water box. **G2-P** scaffold is colored in black, hydrophobic decyl chains in red, hydrophilic PEG in blue, and biotin ligand in green. Oxygen atoms of water molecules are represented as transparent cyan spheres. (b) Final snapshot taken from the MD simulation of **G2-P**. During the MD run all dendrons undergo strong folding in solution assuming a globular shape (R_g = 9.4−10 Å). (c) RDF plots for the G2 dendrons. (d) Simplified model: the dendron−extravidin interaction is composed of two steps: first, unfolding of the biotin ligand (green) that becomes available for the protein at the dendron surface, and second, the specific binding between biotin and extravidin.

was found to increase with increasing concentration of the Myo, as observed with **G1-F** and **G2-F** assemblies. These results are taken to suggest that, since the 0% cross-linked nanogel assembly is quite leaky, Myo itself is not capable of "encapsulating" Nile red molecules in its hydrophobic pockets. This rules out mechanism (i).

The mechanism (ii) can be due to dynamic or static quenching. Since dynamic and static quenching differs in their temperature dependence, we exposed the assemblies **G1-F** and **G2-F** encapsulating Nile red to increasing concentrations of Myo at two different temperatures. The number of collisions between the dendritic assemblies and the protein was expected to increase at a higher temperature as in dynamic quenching, leading to an increase in quenching.[24a] On the other hand, in the case of static quenching, the nonspecific and weak dendritic assembly−protein complex would dissociate at a higher temperature, leading to a decrease in quenching.[24b] Figure S4c,d shows the Stern−Volmer plots for **G1-F** and **G2-F**, respectively, at 25 and 38 °C. The fact that quenching decreases with temperature supports the nonspecific and weakly bound complex hypothesis. Thus, it is interesting to note that **G1-F** and **G2-F** exhibit higher nonspecific interaction and, at the same time, do not exhibit significant release of the guest molecules in response to the target extravidin. On the other hand, the dendrons **G1-P** and **G2-P** that exhibited the highest release in response to extravidin did not exhibit any nonspecific quenching with Myo.

These data and those from the previous sections indicate that if the release of hydrophobic guests is triggered by the specific extravidin−biotin interaction, the selective binding with the complementary protein can occur more easily when a biotin ligand is grafted at the periphery than when it is grafted at the middle layer or at the focal point of the dendron and that this makes the release of hydrophobic guests faster for **G2-P** than for the other constructs, as observed in Figure 3a,b. If disassembly is controlled by the same interaction, since the biotin−extravidin binding is considered irreversible, when extravidin binds to a dendron in the assembly a reduction in the size of assembly will occur after some time, while the system reorganizes and equilibrates in smaller size assemblies, as observed by DLS (Figure 2). Thus, although all systems reorganized into smaller size assemblies, the release was higher for the dendron systems with a ligand located at the periphery. The reason for this disparity was not entirely clear to us.

Based on the release kinetics, which was also faster for the dendritic systems with a ligand at the periphery, we hypothesized that in these cases the assembly reorganization was drastic enough to produce a higher release. On the other hand, in the cases with a ligand at the middle layer and focal point the assemblies rearranged slower into smaller size structures, allowing for the encapsulated hydrophobic small molecules to still be accommodated in hydrophobic pockets. In fact, Figure 3b shows that even after 6 h of **G2-M** (25 μM) exposure to a constant concentration of extravidin (14 μM), the release was as low as 13%. At this point, some interesting questions, including why is the release from **G2-P** so high compared to the release from **G2-M** and **G2-F** remain still open. For this reason, we have employed MD simulations to gain additional insights into this process.

dx.doi.org/10.1021/ja500634u | J. Am. Chem. Soc. 2014, 136, 5385−5399

MD Simulations of the Single Dendrons in Solution. We have used MD simulations focusing on the second generation dendrons in order to understand why the different positioning of a biotin ligand within the dendron scaffold has such a strong effect on the final properties. In particular, we were interested in gaining insight on ligand accessibility from the external solution if it is tethered at the dendron periphery, at the focal point, or at the middle layer. First, it was important to understand what these molecules "look like" in solution. In fact, it is known that similar dendritic structures can undergo strong folding in solution,[25] so that if the biotin ligand is backfolded and surrounded by PEG in the experimental conditions the specific binding with extravidin will be unlikely.

The entire simulation work was carried out with the AMBER 12 suite of programs.[26] Molecular models were created with three different functionalization points for biotin to understand how the individual dendrons arrange in solution. **G2-P**, **G2-F**, and **G2-M** dendron models were created and parametrized according to our similar studies on dendrons interacting with proteins.[27] Starting configurations of the dendrons were then immerged in a simulation box (Figure 4a) containing explicit water molecules (Figure S6 and details in the Supporting Information (SI)). All systems underwent 200 ns of MD in periodic boundary conditions at 25 °C (298 K) of temperature and 1 atm of pressure. During this time, all dendrons reached equilibrium with good stability. The root-mean-square displacement (RMSD) and the radius of gyration (R_g) data extracted from the MD simulations were used to assess the system's equilibration. Computational details for the simulation procedure and data analysis are available in the SI.

Figure 4a shows the starting configuration of **G2-P** immerged in water. Initially, all dendrons were constructed with all PEG chains on one side and all decyl chains on the other side. Molecular models for the G2 dendrons were also constructed with alternated chains to avoid configuration-dependent results. However, MD simulations of those systems suggested that the initial configuration does not have any impact on the shape and equilibrium configuration assumed by such small and flexible molecules in water, in terms of density distribution, radius of gyration, etc. (see Figure S7 and SI for details). These findings are consistent with the idea of treating these dendrons as facially amphiphilic structures.[28]

The size of G2 in water, predicted by MD simulation, does not change substantially depending on the tethering position of biotin; the R_g in the three cases is 9.4−10 Å (Figure 4b). In general, the dendrons tend to compact the hydrophobic decyl chains at the core and to surround them with hydrophilic PEG. On the other hand, in terms of distribution of the biotin ligand the situation is different. The plots in Figure 4c report the radial distribution function $g(r)$ of the biotin ligand calculated with respect to the dendrons center and expressed as a function of the dendron radius (R_g) for the cases where biotin is grafted at the periphery (**G2-P**: red), the middle layer (**G2-M**: blue), or at the focal point (**G2-F**: black). In general, the $g(r)$ values give indication on the relative probability to find the biotin ligand at a certain distance from the dendron center, being the position of the $g(r)$ maximum peak the most probable one. The biotin density going from the center to the surface is calculated at each simulation step, and the reported $g(r)$ data are averaged in time over the equilibrated phase MD trajectories (the last 100 ns). Thus, high and sharp peaks in $g(r)$ identify high biotin density regions, but they also indicate high localization, confinement and backfolding (namely, atoms that cannot move are counted at each step in the same region of space). On the contrary, flexible and fluctuating groups will have low and broad $g(r)$ peaks. Figure 4c shows that at the equilibrium biotin distribution is very different for **G2-P**, **G2-M**, and **G2-F**. In particular, the biotin $g(r)$ maximum peak for **G2-P** (red curve) corresponds well with its R_g indicating that, on average, the ligand availability on the surface is very good. On the contrary, the maximum peaks of black and blue $g(r)$ curves at a distance $r \sim 0.5\ R_g$ suggest that biotin is considerably more backfolded in the case of **G2-F** and **G2-M**.

These data give indication on how much the biotin ligand is available at the surface of the dendron and thus also on the probability to have a specific binding with extravidin. In fact, we built a simplified model describing the dendron−extravidin specific interaction as composed of two phases, namely, the unfolding of the biotin ligand to make it available for the protein and then the specific biotin−avidin interaction (Figure 4d). According to this scheme, we can obtain information on the overall affinity of **G2-P**, **G2-M**, and **G2-F** for extravidin by evaluating the free energy of the dendron-protein binding process as: $\Delta A_{bind} = \Delta A_{specific} + \Delta A_{unfold}$; where the specific biotin−avidin affinity is known experimentally (absolute free energy of binding $\Delta A_{specific} = -20.4$ kcal mol^{-1})[29a,b] and can be considered as a constant for all cases (all dendrons bear the same number of biotin ligands), ΔA_{unfold} is the free energy necessary to drag out the biotin ligand from its backfolded state to make it available at the dendron surface. ΔA_{unfold} values for the different cases can be extracted directly from the $g(r)$[29c] and depend on how much the ligand is backfolded within the dendron structure (details in the SI). In particular, if G2 dendrons are thought of as spheres with radius R_g, $\Delta A_{unfold} = 0$ for **G2-P** as in this case the biotin ligand is most probably available at the dendron surface ($g(r)$ peak position coincides with R_g). On the other hand, for **G2-F** and **G2-M** ΔA_{unfold} is an unfavorable term (>0) that depends on the level of backfolding, namely, the lower the biotin ligand availability at the surface (high level of backfolding), the higher the necessary free energy to make it available at the dendrons' surface for avidin binding. Table 1 reports the free energy of binding values calculated for the different dendrons.

Table 1. Free Energy Values for the Dendron−Extravidin Interaction[a]

dendron	ΔA_{unfold}[b]	$\Delta A_{specific}$[c]	ΔA_{bind}[d]	statistical weight[e]
G2-P	0	−20.4	−20.4	1
G2-M	1.40	−20.4	−19.0	0.097
G2-F	1.38	−20.4	−19.02	0.10

[a]Data are expressed in kcal mol^{-1}. [b]ΔA_{unfold} depends on the level of ligand backfolding. It can be calculated for all cases directly from the $g(r)$; see SI. [c]Experimental biotin−avidin affinity − $\Delta A_{specific}$ = −20.4 kcal mol^{-1}.[28a,b] [d]Global dendron−avidin binding affinity was calculated as: $\Delta A_{bind} = \Delta A_{specific} + \Delta A_{unfold}$. [e]Relative probability for the dendron−avidin specific interaction (statistical weight) can be calculated as $\exp(-\Delta A_{bind} k_b T^{-1})$.

We also calculated the statistical weight for the different dendrons from the dendron−avidin affinity energies as $\exp(-\Delta A_{bind}\ k_b T^{-1})$ (k_bT = 0.593 kcal mol^{-1} at room temperature), which provides qualitative indication on the relative probability for a specific binding with extravidin in the case of **G2-P**, **G2-M**, and **G2-F**, depending on how much the biotin ligand is available at the surface. In particular, these data

dx.doi.org/10.1021/ja500634u | J. Am. Chem. Soc. 2014, 136, 5385−5399

suggest that if we set the probability of having extravidin specifically bound to the biotin moiety in **G2-P** to 1, then the probability of having extravidin bound to the biotin moiety in **G2-F** and **G2-M** is reduced to ∼0.1 due to reduced ligand availability; a difference of 1 order of magnitude indicating that the extravidin specific binding to biotin ligands from the dendrons at the surface of **G2-P** aggregates is 10 times higher than in the case of **G2-F** and **G2-M**. We will come back to this important point in the next sections.

Modeling the Specific Binding between G2-P and Avidin. Then we aimed at studying the specific binding between one dendron and extravidin. Since we did not have any information regarding the conformation assumed by the dendron during the binding with extravidin, we started from the unfolded configuration of one dendron (Figure 5d).

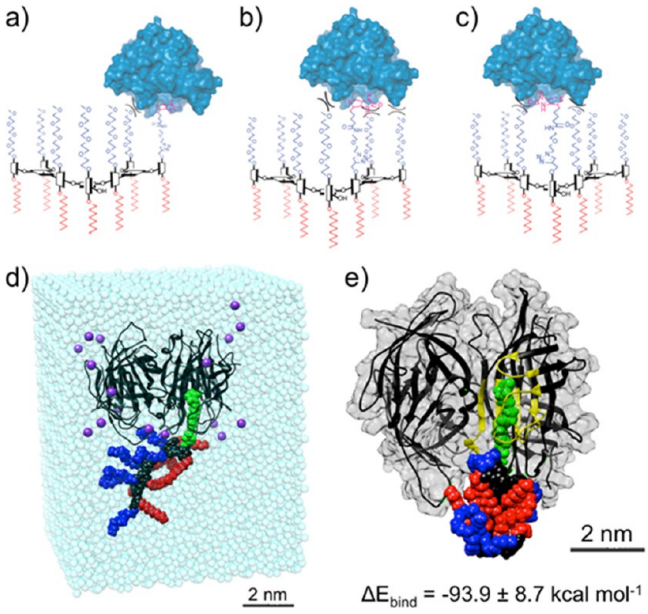

Figure 5. Dendron-extravidin specific binding. (a) When biotin is tethered at the periphery, it is more available for extravidin binding. On the contrary, when it is grafted at the middle layer (b) or at the focal point (c), it is surrounded by an environment rich in PEG, so that the deep penetration of the ligand in one of the binding pockets of extravidin is hindered. (d) Starting configuration of the **G2-P+AVD** molecular system. **G2-P** backbone is colored in black, hydrophobic decyl chains in red, hydrophilic PEG in blue, and biotin in green. Oxygen atoms of water molecules and Cl^- counterions are represented as transparent cyan and purple spheres, respectively. Extravidin is represented as a black ribbon. (e) Last equilibrated snapshot taken from the MD simulation of the **G2-P+AVD** system. During the MD run the specific binding between biotin and extravidin remained very stable. Extravidin binding pocket is colored in yellow, and water molecules and counterions are not shown for clarity.

Initially, the biotin ligand of one unfolded **G2-P** was superimposed to the native biotin present in chain A of the crystallographic structure for the extravidin tetramer (PDB: 1AVD) replacing it and thus obtaining the first **G2-P+AVD** molecular complex.

When biotin is grafted at the middle layer (Figure 5b) or the focal point (Figure 5c) it is surrounded by an environment rich in PEG. This makes the specific binding with extravidin, which implies the deep penetration of the ligand inside one of the four binding pockets of tetrameric extravidin, very difficult compared to **G2-P** (Figure 5a). This difficulty was reflected also on modeling. In fact, it was not possible to create the initial complex with extravidin for **G2-F** and **G2-M** without incurring intractable distortions. For this reason and in light of the results on biotin availability discussed in the previous section, for what pertains to the modeling study of the interactions with the complementary protein, we focused only on **G2-P**.

The starting configuration of the **G2-P+AVD** complex (Figure 5d) was immerged in a periodic box containing explicit water molecules and the minimum number of counterions necessary to guarantee the system neutrality (details in the SI). **G2-P+AVD** system was equilibrated for 200 ns of NPT MD simulation at 25 °C (298 K) and 1 atm of pressure. This time was sufficient to reach the equilibrium. During the MD run, the binding between biotin and extravidin remained very strong and stable (see SI for details). The interaction energy (ΔE_{bind}) between **G2-P** and extravidin was extracted directly from the MD trajectories according to the MM-PBSA approach.[30] In particular, ΔE_{bind} is the sum of the gas-phase *in vacuo* interaction energy (ΔE_{gas}) and the solvation term (ΔE_{sol}). In general, the more negative the ΔE_{bind} value, the stronger the binding. In the case of a 1:1 binding between **G2-P** and extravidin, ΔE_{bind} was calculated to be as strong as -93.9 ± 8.7 kcal mol^{-1} at the equilibrium.

Modeling G2-P Self-Assembly and Extravidin Binding-Induced Disassembly. In our preliminary communication, we had suggested that the change in hydrophilic−lipophilic balance upon protein binding likely drives the binding-induced disassembly.[13a] To further test this hypothesis, we first modeled the amphiphilic assembly of **G2-P** dendrons in water. Then, we aimed at understanding how the dendron assembly changes upon extravidin addition to the system.

MD simulation allows for the study of hydrophobic aggregation in water, as it was recently reported in the case of the self-assembly of hydrophobic drug molecules and amphiphilic diblock copolymer micelles.[31] According to the same protocol, nine copies of **G2-P** dendron arranged on a plane were immerged in a simulation box filled with explicit water molecules. In particular, as a starting configuration for the **G2-P** dendron (Figure 6a), we chose the final equilibrated configuration produced by the simulation of **G2-P+AVD** binding (Figure 5e), with the biotin ligand initially extended in extravidin-bound conformation, so that it was also possible to add a bound extravidin to the central dendron without difficulties. We thus generated two molecular systems both containing nine **G2-P** dendrons solvated in water, where the central dendron is respectively unbound (Figure 6a: **9G2-P**) or bound to one extravidin protein (Figure 6c; **9G2-P+AVD**), in such a case the central dendron was simply replaced by the **G2-P+AVD** complex from Figure 5e.

Both systems were equilibrated for 200 ns of MD simulation at 25 °C and 1 atm pressure. During the simulation of the **9G2-P** system, we found that the nine dendrons by themselves showed a strong propensity to self-assemble. The aggregate also reorganized in order to decrease the exposure of the hydrophobic regions (red) to the external solution. In general, Figure 6b shows that the red decyl chains converge at the core of the aggregate and are surrounded by blue PEG chains. Biotin ligands (green) are well exposed to the surface. Structural reorganization during self-assembly is also demonstrated by the R_g plots in Figure 6e obtained from the MD simulation of the **9G2-P** system. Red decyl chains converge to a lower R_g value than PEG (blue) and biotin (green), indicating structural reorganization within the aggregate due to hydrophobic effects.

dx.doi.org/10.1021/ja500634u | J. Am. Chem. Soc. 2014, 136, 5385−5399

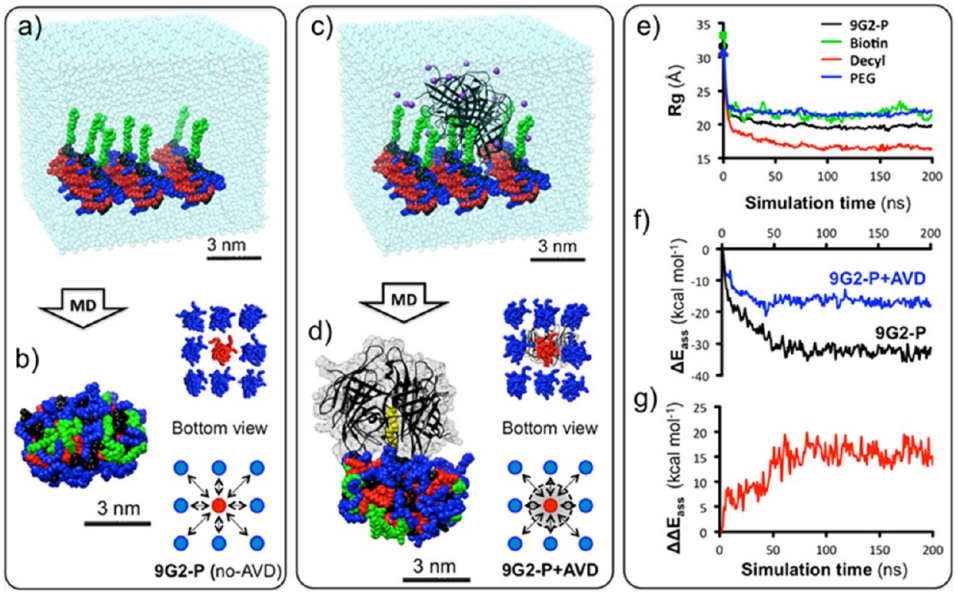

Figure 6. **G2-P** self-assembly and extravidin-induced disassembly. (a) Initially, nine copies of unbound **G2-P** dendrons were immerged in a simulation box containing water (**9G2-P** system). (b) During 200 ns of MD simulation the nine dendrons aggregate and rearrange: hydrophilic PEG (blue) and biotins (green) surround the hydrophobic parts (red decyl chains). (c) The starting configuration for the **G2-P+AVD** system is the same of **G2-P**, but a tetrameric extravidin protein (AVD: black ribbons) is bound to the central **G2-P** dendron. Cl^- ions (purple) were also added for neutralization. (d) The **9G2-P+AVD** system was equilibrated for 200 ns of MD simulation, during which the specific binding between biotin (yellow) and AVD remains stable and the nine **G2-P** dendrons in the system self-assemble. (e) R_g plots for the **9G2-P** assembly case (black curve). R_g plots are obtained also for the biotin ligands (green), PEG (blue), and hydrophobic decyl chains (red) to understand molecular reorganization in solution. (f) The central dendron (b,d: red) was used as a reference, and the self-assembly energy (ΔE_{ass}) was extracted for the MD simulations. ΔE_{ass} values were obtained for the **9G2-P** (black) and **9G2-P+AVD** (blue) systems and plotted as a function of simulation time. (g) The energetic difference $\Delta\Delta E_{ass}$ (red) identifies the **G2-P** self-assembly destabilization due to AVD binding.

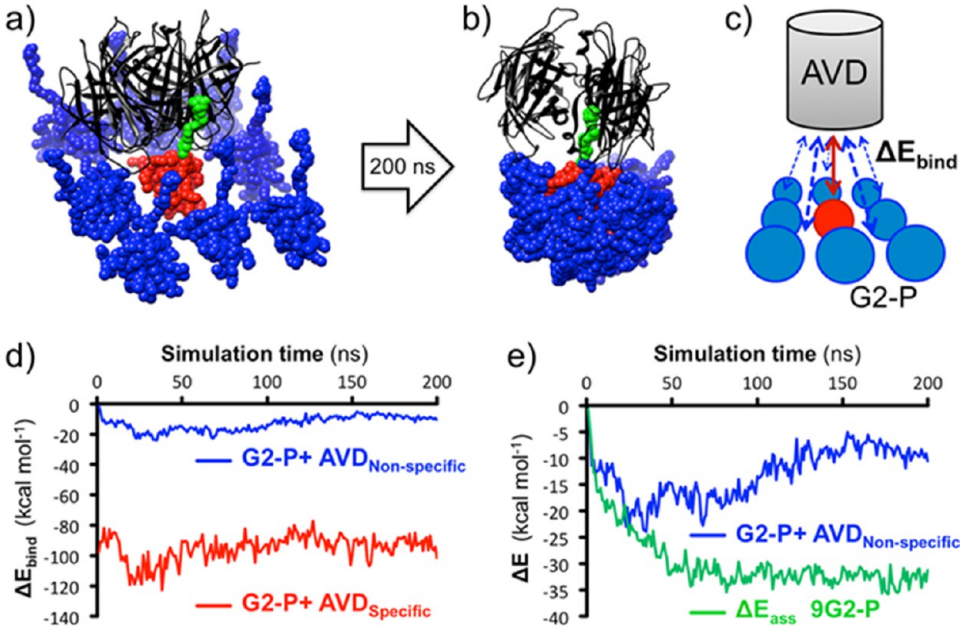

Figure 7. Specific and nonspecific interaction at the interface between AVD and **G2-P** aggregates. (a,b) During the MD simulation the dendrons self-assemble and blue dendrons surround the red one, which is specifically bound to AVD (biotin in green). (c) The dendrons can interact with extravidin specifically (red) and also nonspecifically (blue). (d) Specific (red) and nonspecific (blue) interaction energies normalized per dendron expressed as a function of simulation time. (e) Nonspecific interactions with AVD (blue) are sensibly lower than the dendrons native self-assembly energy (green, the same **9G2-P** values reported in black in Figure 6f), demonstrating why nonspecific interactions alone are energetically not strong enough to trigger disassembly.

Similar aggregation occurred also in the **9G2-P+AVD** system containing eight **G2-P** unbound dendrons surrounding a single **G2-P+AVD** complex (Figure 6c,d). However, interestingly in this case the aggregate was clearly less tight and less ordered at the equilibrium than in the **9G2-P** case. We were interested in evaluating the native propensity of **G2-P** dendrons to self-

dx.doi.org/10.1021/ja500634u | J. Am. Chem. Soc. 2014, 136, 5385−5399

assemble and in understanding how much the latter is affected when one specific binding with a complementary protein occurs at the surface of the aggregate. Thus, we obtained from the MD simulations the dendrons self-assembly energy (ΔE_{ass}) for the two systems. The latter was evaluated as the binding energy between the central dendron with the other eight surrounding ones in the systems (schemes in Figure 6b,d: red and blue dendrons, respectively).[15c] ΔE_{ass} was calculated as described in the previous section, taking into account for solute−solute and solute−solvent interactions (details on energetic analysis in the SI). ΔE_{ass} calculated values were further normalized per dendron (i.e., divided per 8), so that they become general indicators of how stable is the aggregation within the **G2-P** aggregates.

Data reported in Figure 6f show that, at the equilibrium, the self-assembly energy triggering aggregation is as high as $\Delta E_{ass} = -32.5 \pm 1.4$ kcal mol^{-1} in absence of extravidin binding (**9G2-P**: black curve). On the other hand, in the **9G2-P+AVD** system ΔE_{ass} is reduced to -16.8 ± 1.4 kcal mol^{-1} (blue curve). The destabilization induced by the specific binding with extravidin is represented by the energetic difference $\Delta\Delta E_{ass} = \Delta E_{ass}$ (**9G2-P+AVD**) − ΔE_{ass} (**9G2-P**). Positive values for $\Delta\Delta E_{ass}$ indicate that, in general, when an AVD protein binds specifically to one biotin ligand at the surface of a **G2-P** aggregate, the self-assembly is locally destabilized, which could be the trigger for disassembly. In our case, the energetic destabilization due to extravidin binding converged to the value of $\Delta\Delta E_{ass} = +15.7 \pm 1.7$ kcal mol^{-1} (Figure 6g, red curve), indicating that when one AVD binding occurs, the stability of **G2-P** dendron self-assembly (ΔE_{ass}) is reduced to the half.

We also extracted useful information from the MD simulations regarding specific and nonspecific interactions (Figure 7). In fact, during the 200 ns of MD simulation of the **9G2-P+AVD** system, we saw that all nine **G2-P** dendrons interact not only with each other but also with extravidin (Figure 7a−c). Importantly, while the central dendron (red) is specifically bound to the protein through the biotin ligand, the other eight interact with AVD nonspecifically. To obtain insights into the differences between specific and nonspecific interactions with AVD, we extracted the binding energy (ΔE_{bind}) between the dendron aggregate and extravidin from the MD simulation of **9G2-P+AVD** through the same approach adopted previously. ΔE_{bind} measures the global interaction of the aggregate (composed of nine dendrons) for AVD, and it was calculated as $\Delta E_{bind} = -162.5 \pm 14.3$ kcal mol^{-1}, equivalent to $\Delta E_{bind} = -18.1 \pm 1.6$ kcal mol^{-1} per dendron, at the equilibrium. Thus, this result shows that in general extravidin is attracted by **G2-P** aggregates, which suggests that as soon as extravidin is added to a solution containing dendron aggregates there will be a long-range trigger for molecular recognition.

How much of this attraction is due to the specific interaction (red dendron) and how much to nonspecific interactions? We obtained this information *via* a simple decomposition of the global ΔE_{bind} energy on a per dendron basis. This analysis shows that most of the interaction is due to the specific binding between the red dendron in Figure 7 and AVD, that is as strong as $\Delta E_{bind} = -91.6 \pm 5.4$ kcal mol^{-1}. Such a high ΔE_{bind} value is very close to that found for the 1:1 **G2-P+AVD** binding in Figure 5, which demonstrates that the presence of the other blue dendrons in the aggregate does not affect the strength of the specific binding. On the other hand, nonspecific interactions with extravidin are on average sensibly lower ($\Delta E_{bind} = -8.8 \pm 1.9$ kcal mol^{-1}). This result shows that in this case the strength of nonspecific interactions is 1 order of magnitude weaker than specific interactions and also less persistent and more discontinuous, as demonstrated by the standard deviation which is ∼20% of the ΔE_{bind} average value (for specific interactions the latter is ∼6%). Interestingly, nonspecific interactions, even if present, are weaker than the intrinsic self-assembly energy of **G2-P** dendrons (Figure 7e: ∼9 vs. ∼33 kcal mol^{-1}). For this reason, they are probably not strong enough to perturb the stability of the aggregates, which is consistent with our DLS evidence (Figure 2) showing no disassembly in the case of noncomplementary proteins.

Multivalent AVD Binding. All these results suggest that as soon as extravidin gets in contact with the surface of a **G2-P** aggregate, the formation of a specific binding will be an energetically favored event. In addition, it is worth noting that extravidin is a protein tetramer possessing four binding sites for biotin. Thus, after a first specific binding occurs between AVD with one biotin at the **G2-P** aggregate surface, the protein can find also other biotin ligands available in the neighborhood to establish many more specific bindings in a cooperative way. According to the so-called multivalent effect, this will be an energetically favored thus highly probable event.[32]

To test this hypothesis, we performed the MD simulation, similar to that in Figure 5, but with four **G2-P** dendrimers bound to all of the biotin binding sites of tetrameric AVD (Figure 8a,b). The result of the energetic analysis for this case is

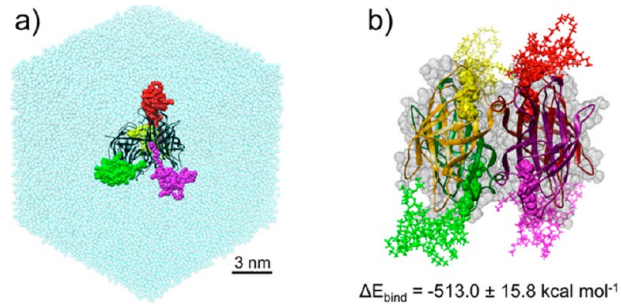

Figure 8. Multivalent AVD binding. (a) An additional system was simulated with four **G2-P** dendrons (yellow, green, magenta, and red) specifically bound to the four biotin binding sites of extravidin (PDB: 1AVD). (b) Binding energy extracted from this MD simulation indicates that the specific binding of AVD to multiple **G2-P** dendrons is energetically favored.

in agreement with the multivalency principle. In fact, the interaction energy (ΔE_{bind}) between AVD and all four **G2-P** dendrons extracted from this simulation and reported in Figure 8b is sensibly higher than that related to the binding of a single dendron reported in Figure 5 (multiplied per four, which equals to: $\Delta E_{bind} = -375.6 \pm 34.9$ kcal mol^{-1}). This large difference of ∼137 kcal mol^{-1} is a clear signal of multivalency, and it demonstrates that AVD is energetically favored to bind more biotins at the same time.

The consequences of this behavior can be important. In fact, this tendency of AVD to bind more biotin ligands at the same time, when available, can in principle speed up the disassembly process. Conceptually, since AVD will tend to preserve its structure much more than the dendron aggregate, in the case of cooperative binding to multiple ligands, it is reasonable to think that the dendrons from the aggregate will adapt over extravidin, rather than the contrary (unlikely protein collapsing over the

dx.doi.org/10.1021/ja500634u | J. Am. Chem. Soc. 2014, 136, 5385−5399

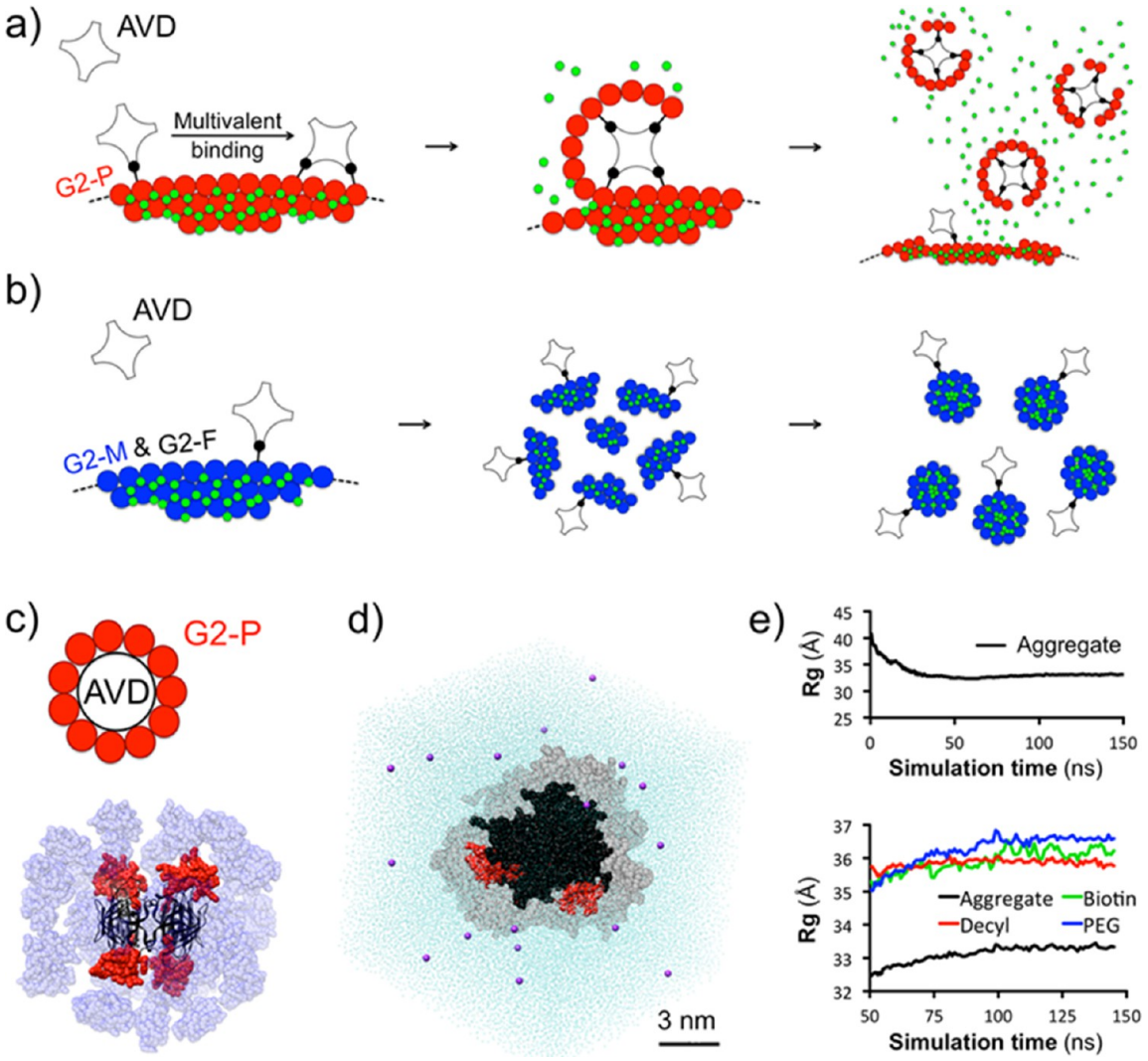

Figure 9. Proposed mechanisms for disassembly. (a) Due to high biotin availability at the surface of **G2-P** (red) aggregates, the formation of multivalent AVD-biotin bindings is an energetically favored phenomenon. While completing multiple bindings, AVD would trigger the fast disassembly of the aggregates into small aggregates (AVD micelles) via exfoliation, leading to the release of hydrophobic fluorescent guest molecules in solution (green). (b) On the other hand, even if a less favored specific binding event occurs at the surface of **G2-M** and **G2-F** aggregates (blue), multivalent binding of the same AVD to multiple biotins is unlikely due to low ligand availability. The dendron aggregates would disassemble in larger and more ordered assemblies that would be able to retain the guests in their interior. (c) Starting configuration of an additional system containing one AVD (black ribbons) with four specific bindings with four **G2-P** dendrons (red) and surrounded by other 36 **G2-P** dendrons (transparent blue). The number of **G2-P** dendrons that can surround one AVD being in contact with the surface was calculated as ∼40 according to the Mansfield−Tomalia−Rakesh equation.[32] (d) Final snapshot of the MD simulation of the large aggregate in solution (oxygen atoms of water molecules in transparent cyan and counterions in purple). During the simulation all **G2-P** dendrons (transparent black) collapse and surround AVD (black). Specifically bound dendrons are colored in red. (e) Gyration radius of the large aggregate over simulation time (black). During the MD run the dendrimers first aggregate around AVD and then undergo rearrangement, surrounding the hydrophobic decyl chains (red) with the hydrophilic PEG chains (blue). R_g plots for biotin ligands are represented in green.

G2-P surface). This is consistent with a picture where **G2-P** aggregates are progressively degraded.

Two Different Proposed Mechanisms for Disassembly. One key factor allowing for multivalent binding is biotin availability, i.e., biotin ligands must be accessible at the aggregate surface and free to complete specific interactions with AVD. In fact, as we already discussed with Figure 4c,d, the chance of having multivalent binding between the dendrons with AVD will be extremely sensitive to biotin availability at the surface of the aggregates. Our MD simulations suggested that biotin availability is high for **G2-P** and low for **G2-M** and **G2-F** (Figure 4c,d). Thus, at the **G2-P** aggregates surface AVD will find many accessible binding spots for completing specific interactions. Moreover, after a first specific binding is established, the same AVD protein will be then energetically favored to bind more biotins from other **G2-P** dendrons. On the other hand, since the probability to have specific binding for **G2-M** and **G2-F** is reduced, even if a first specific interaction occurs between AVD and one biotin ligand, it is reasonable to hypothesize that the chance of having multivalent AVD binding at the surface of **G2-M** and **G2-F** aggregates will be even lower.

In light of these results, we propose two possible mechanisms for the observed supramolecular disassembly (schematized in Figure 9). A first one for the **G2-P** case based on multivalent binding of AVD, leading to the rapid disassembly of the dendron aggregates in solution due to exfoliation (Figure 9a). A

dx.doi.org/10.1021/ja500634u | J. Am. Chem. Soc. 2014, 136, 5385−5399

second one for **G2-M** and **G2-F**, where the aggregates would disassemble more slowly due to the destabilization (Figure 6) induced by the specific binding with AVD (Figure 9b). In principle, the first mechanism would result in the rapid production of smaller aggregates (since they are limited by AVD size) and in a higher level of hydrophobic guests release. In fact, the velocity of the process and the small size of the aggregates would not allow for the structural rearrangement necessary to retain the guest molecules. The second proposed mechanism would most likely produce larger size aggregates and lower levels of release.

This hypothesis is consistent with all our experimental evidence. In fact, the high level of biotin availability of **G2-P** (Figure 4c,d) is compatible with the fast disassembly and hydrophobic guests release by **G2-P** aggregates in presence of extravidin, as shown by our DLS and fluorescence experiments. At the same time, our data demonstrate that **G2-M** and **G2-F** aggregates also disassemble in presence of extravidin (Figure 2), but more slowly. In addition, the final size of the disassembled aggregates is larger than that of **G2-P** (∼14 VS ∼7 nm), and no appreciable guest release is present during the disassembly of the **G2-M** and **G2-F** aggregates (Figure 3). Finally, we performed another MD simulation aiming at representing the final step of the disassembly mechanism based on multivalent binding and exfoliation represented in Figure 9a.

First, we calculated how many **G2-P** dendrons, thought of as small spheres, would be necessary to surround completely an AVD molecule, thought of as a larger sphere, while being in direct contact with the protein surface. Using the gyration radii of a single **G2-P** dendron and AVD obtained from our MD simulations (respectively, R_g = 0.97 and 2.2 nm on average), we found that in our case this ratio equals to ∼40 **G2-P** dendrons for a single AVD according to the Mansfield−Tomalia−Rakesh equation.[33] Then we started from the final configuration obtained from the simulation of AVD specifically bound to four **G2-P** dendrons and have added other 36 equilibrated **G2-P** dendrons surrounding the complex (Figure 9c). The system was then immerged in a simulation box containing explicit solvent molecules and simulated for 150 ns in NPT conditions, at 25 °C of temperature and 1 atm of pressure. During this time, all 40 **G2-P** dendrons collapsed over the surface of AVD surrounding the protein (Figure 9d) and forming a real protein micelle.[34] Furthermore, during the MD simulation the entire aggregate underwent structural reorganization attempting to surround the surface with hydrophilic PEG, limiting as much as possible the exposure of the hydrophobic parts to water. This structural rearrangement is testified by the R_g plots of Figure 9e, demonstrating how during the MD simulation the PEG chains surround the surface of the aggregate. We also calculated the equilibrated size of the whole aggregate of Figure 9d, which resulted to be R_g = 3.3 nm. Considering the compact and globular nature of this large aggregate, the hydrodynamic size can be calculated as $R_h \sim 1.29\ R_g$.[25a] For this case the obtained size is thus $D_h \sim 8.5$ nm, which is in good agreement with the size obtained for the disassembled aggregates in the case of **G2-P** (Figure 2).

CONCLUSIONS

Our research reveals that ligand placement on a supramolecular scaffold for binding-induced disassembly greatly impacts disassembly and release of encapsulated guest molecules, as we have shown from the high release difference observed, for example, between **G2-P** and **G2-M**. The best place to attach a ligand, looking for a protein triggered release from a dendritic micelle-like nanostructure, is the periphery. MD simulations show backfolding of the ligand, when attached to middle layer and focal point; and a better availability for protein binding, when the ligand is attached at the periphery. Incorporation of the biotin ligand in the dendrons gives the dendritic assemblies selectivity toward the target protein extravidin, regardless of the ligand position. Nonetheless, ligand positioning in the dendrons gives the assemblies sensitivity toward release upon binding of a target protein. MD simulations show that after AVD binding the stability of **G2-P** assembly is strongly affected, possible signal of AVD binding-induced disassembly. In addition, our computational efforts show that once a first specific binding between AVD and one **G2-P** dendron occurs, the multivalent binding of the same protein to other **G2-P** dendrons via specific biotin−extravidin interaction is an energetically favored event. This evidence allowed us to hypothesize two different mechanisms of disassembly induced by AVD binding. The divergence of the mechanism also allows us to explain the observed experimental differences in guest release that depend on the ligand location in the scaffold. A fast one for **G2-P** based on high biotin availability at the aggregate surface, multivalent interactions, and aggregates exfoliation. This mechanism leads to fast formation of small disassembled aggregates and to a high release of hydrophobic guests. A second mechanism for **G2-M** and **G2-P**, slower, based on AVD binding-induced aggregate destabilization and producing larger and more ordered aggregates in solution that are still capable of retaining the guest molecules in their interior.

Substitution of a PEG unit in the dendrimer with a pendant biotin increased nonspecific interactions of the assemblies with proteins, which was seen as the formation of larger aggregates in solution. This became more evident when the density of PEG chains on the hydrophilic face was low, as it is in a G1 dendron compared to a G2. This, in turn, facilitates the formation of a weak complex with proteins, which was evidenced when a metalloprotein acted as a quencher, generating static quenching of the encapsulated fluorophore molecules. The combination of these results shows that G2 dendrons are better for selectivity and that the periphery is the best location for achieving binding-induced disassembly. Thus, **G2-P** exhibits most guest release and least nonspecific interactions with other proteins. Our MD simulations of **G2-P** show that, despite the general affinity between the aggregates and AVD, nonspecific interactions alone are too weak, and a specific binding (more than 1 order of magnitude stronger) is needed to trigger the release of the hydrophobic guest molecules. The research reported here gives a picture of how supramolecular disassembly and release might be largely affected by choosing a specific location for a trigger, rather than a random placement based on molecular architecture. Also, we have shown how controlled variations in PEG density could affect interactions of nanoparticles with proteins. Developing zwitterionic moieties,[35] which have the potential to circumvent the steric hindrance exhibited by lengthy PEG chains in amphiphilic systems, for use in protein-binding-induced disassembly is part of the ongoing focus in our laboratories.

ASSOCIATED CONTENT

Supporting Information

Synthetic procedures and data from NMR, MS, fluorescence, and DLS. Details about computational procedures and MD

dx.doi.org/10.1021/ja500634u | J. Am. Chem. Soc. 2014, 136, 5385−5399

additional data. This material is available free of charge via the Internet at http://pubs.acs.org.

AUTHOR INFORMATION

Corresponding Authors

thai@chem.umass.edu
giovanni.pavan@supsi.ch

Notes

The authors declare no competing financial interest.

ACKNOWLEDGMENTS

Support from NIGMS of the National Institutes of Health (GM-065255) is gratefully acknowledged.

REFERENCES

(1) (a) Sorrenti, A.; Illa, O.; Ortuño, R. M. *Chem. Soc. Rev.* **2013**, *42*, 8200−8219. (b) Zhao, Y.; Sakai, F.; Su, L.; Yijiang, L.; Wei, K.; Chen, G.; Jiang, M. *Adv. Mater.* **2013**, *25*, 5215−5256. (c) Busseron, E.; Ruff, Y.; Moulin, E.; Giuseppone, N. *Nanoscale* **2013**, *5*, 7098−7140. (d) Bai, C.; Liu, M. *Angew. Chem., Int. Ed.* **2013**, *52*, 2678−2683.

(2) (a) Almutairi, A.; Guillaudeu, S. J.; Berezin, M. J.; Achilefu, S.; Fréchet, J. M. J. *J. Am. Chem. Soc.* **2008**, *130*, 444−445. (b) Qiao, Z.; Ji, R.; Huang, X.; Du, F.; Zhang, R.; Liang, D.; Li, Z. *Biomacromolecules* **2013**, *14*, 1555−1563.

(3) (a) Zhang, H.; Shen, J.; Liu, Z.; Hao, A.; Bai, Y.; An, W. *Supramol. Chem.* **2010**, *22*, 297−310. (b) Wang, Y.; Xu, H.; Zhang, X. *Adv. Mater.* **2009**, *21*, 2849−2864.

(4) (a) Yesilyurt, V.; Ramireddy, R.; Thayumanavan, S. *Angew. Chem., Int. Ed.* **2011**, *50*, 3038−3042. (b) Raghupathi, K. R.; Azagarsamy, M. A.; Thayumanavan, S. *Chem.—Eur. J.* **2011**, *17*, 11752−11760.

(5) (a) Kojima, C.; Tsumura, S.; Harada, A.; Kono, K. *J. Am. Chem. Soc.* **2009**, *131*, 6052−6053. (b) Huang, X.; Du, F.; Cheng, J.; Dong, Y.; Liang, D.; Ji, S.; Lin, S.; Li, Z. *Macromolecules* **2009**, *42*, 783−790. (c) Li, Y.; Lokitz, B. S.; McCormick, C. *Angew. Chem., Int. Ed.* **2006**, *45*, 5792−5795.

(6) (a) Meng, F.; Zhong, Z.; Feijen, J. *Biomacromolecules* **2009**, *10*, 197−209. (b) Nam, J.-M.; Thaxton, C. S.; Mirkin, C. A. *Science* **2003**, *301*, 1884−1886.

(7) (a) da Silva Cardeal, L. B.; Boccardo, E.; Termini, L.; Rabachini, T.; Andreoli, M. A.; di Loreto, C.; Filho, A. L.; Villa, L. L.; Maria-Engler, S. S. *PLoS One* **2012**, *7*, e33585. (b) Hayes, G. M.; Carrigan, P. E.; Miller, L. J. *Cancer Res.* **2007**, *67*, 2072−2080. (c) Mao, J.-H.; Kim, I.-J.; Wu, D.; Climent, J.; Kang, H. C.; DelRosario, R.; Balmain, A. *Science* **2008**, *321*, 1499−1502.

(8) (a) Mintzer, M. A.; Grinstaff, M. W. *Chem. Soc. Rev.* **2011**, *40*, 173−190. (b) Chan, D. P. Y.; Owen, S. C.; Shoichet, M. S. *Bioconjugate Chem.* **2013**, *24*, 105−113. (c) Ramireddy, R. R.; Raghupathi, K. R.; Amado Torres, D.; Thayumanavan, S. *New J. Chem.* **2012**, *36*, 340−349. (d) Lee, C. C.; MacKay, J. A.; Fréchet, J. M. J.; Szoka, F. C. *Nat. Biotechnol.* **2005**, *23*, 1517−1526. (e) Tomalia, D. A.; Reyna, L. A.; Svenson, S. *Biochem. Soc. Trans.* **2007**, *35*, 61−67. (f) Patri, A. K.; Kukowska-Latallo, J. F.; Baker, J. R., Jr. *Adv. Drug Delivery Rev.* **2005**, *57*, 2203−2214. (g) D'Emanuele, A.; Attwood, D. *Adv. Drug Delivery Rev.* **2005**, *57*, 2147−2162. (h) Kojima, C. *Expert Opin. Drug Delivery* **2010**, *7*, 307−319.

(9) (a) Yamaguchi, N.; Zhang, L.; Chae, B.-S.; Palla, C. S.; Furst, E. M.; Kiick, K. L. *J. Am. Chem. Soc.* **2007**, *129*, 3040−3041. (b) Saha, K.; Agasti, S. S.; Kim, C.; Li, X.; Rotello, V. M. *Chem. Rev.* **2012**, *112*, 2739−2779.

(10) (a) Amir, R. J.; Zhong, S.; Pochan, D. J.; Hawker, C. J. *J. Am. Chem. Soc.* **2009**, *131*, 13949−13951. (b) Azagarsamy, M. A.; Sokkalingam, P.; Thayumanavan, S. *J. Am. Chem. Soc.* **2009**, *131*, 14184−14185.

(11) (a) Savariar, E. N.; Ghosh, S.; González, D. C.; Thayumanavan, S. *J. Am. Chem. Soc.* **2008**, *130*, 5416−5417. (b) Abdelkebir, K.; Gaudière, F.; Morin-Grognet, S.; Coquerel, G.; Atmani, H.; Labat, B.; Ladam, G. *Langmuir* **2011**, *27*, 14370−14379. (c) González, D. C.; Savariar, E. N.; Thayumanavan, S. *J. Am. Chem. Soc.* **2009**, *131*, 7708−7716.

(12) (a) Wang, F.; Gomez-Escudero, A.; Ramireddy, R. R.; Murage, G.; Thayumanavan, S.; Vachet, R. *J. Am. Chem. Soc.* **2013**, *135*, 14179−14188. (b) Rodthongkum, N.; Ramireddy, R. R.; Thayumanavan, S.; Vachet, R. *Analyst* **2012**, *137*, 1024−1030. (c) Rodthongkum, N.; Chen, Y.; Thayumanavan, S.; Vachet, R. *Anal. Chem.* **2010**, *82*, 8686−8691. (d) Gomez-Escudero, A.; Azagarsamy, M. A.; Theddu, N.; Vachet, R. W.; Thayumanavan, S. *J. Am. Chem. Soc.* **2008**, *130*, 11156−11163. (e) Combariza, M. Y.; Savariar, E. N.; Vutukuri, D. R.; Thayumanavan, S.; Vachet, R. W. *Anal. Chem.* **2007**, *79*, 7124−7130. (f) Reference 28.

(13) (a) Azagarsamy, M. A.; Yesilyurt, V.; Thayumanavan, S. *J. Am. Chem. Soc.* **2010**, *132*, 4550−4551. (b) Guo, J.; Chen, G.; Ning, X.; Wolfert, M. A.; Li, X.; Xu, B.; Boons, G.-J. *Chem.—Eur. J.* **2010**, *16*, 13330−13366. (c) Takaoka, Y.; Sakamoto, T.; Tsukiji, S.; Narazaki, M.; Matsuda, T.; Tochio, H.; Shirakawa, M.; Hamachi, I. *Nat. Chem.* **2009**, *1*, 557−561. (d) Mizusawa, K.; Ishida, Y.; Takaoka, Y.; Miyagawa, M.; Tsukiji, S.; Hamachi, I. *J. Am. Chem. Soc.* **2010**, *132*, 7291−7293. (e) Mizusawa, K.; Takaoka, Y.; Hamachi, I. *J. Am. Chem. Soc.* **2012**, *134*, 13386−13395. (f) Yesilyurt, V.; Ramireddy, R.; Azagarsamy, M. A.; Thayumanavan, S. *Chem.—Eur. J.* **2012**, *18*, 223−229.

(14) (a) Grayson, S. M.; Fréchet, J. M. J. *Chem. Rev.* **2001**, *101*, 3819−3867. (b) Astruc, D.; Boisselier, E.; Ornelas, C. *Chem. Rev.* **2010**, *110*, 1857−1959. (c) Tomalia, D. A.; Fréchet, J. M. J. *J. Polym. Sci., Polym. Chem.* **2002**, *40*, 2719−2728. (d) Tully, D. C.; Fréchet, J. M. J. *Chem. Commun.* **2001**, *37*, 1229−1239.

(15) (a) Bo, Z.; Schäfer, A.; Franke, P.; Schlüter, D. *Org. Lett.* **2000**, *2*, 1645−1648. (b) Azagarsamy, M. A.; Krishnamoorthy, K.; Sivanandan, K.; Thayumanavan, S. *J. Org. Chem.* **2009**, *74*, 9475−9485. (c) Sivanandan, K.; Aathimanikandan, S. V.; Arges, C. G.; Bardeen, C. J.; Thayumanavan, S. *J. Am. Chem. Soc.* **2005**, *127*, 2020−2021. (d) Sivanandan, K.; Britto, S. S.; Thayumanavan, S. *J. Org. Chem.* **2004**, *69*, 2937−2944. (e) Lee, C.; Lo, S.-T.; Lim, J.; da Costa, V. C. P.; Ramezani, S.; Öz, O. K.; Pavan, G. M.; Annunziata, O.; Sun, X.; Simanek, E. E. *Mol. Pharmaceutics* **2013**, *10*, 4452−4461.

(16) (a) Cheng, Y.; Ho, D. M.; Gottlieb, C. R.; Kahne, D. *J. Am. Chem. Soc.* **1992**, *114*, 7319−7320. (b) McQuade, D. T.; Barrett, D. G.; Desper, J. M.; Hayashi, R. K.; Gellman, S. H. *J. Am. Chem. Soc.* **1995**, *117*, 4862−4869.

(17) (a) Bharathi, P.; Zhao, H.; Thayumanavan, S. *Org. Lett.* **2001**, *3*, 1961−1964. (b) Vutukuri, D. R.; Basu, S.; Thayumanavan, S. *J. Am. Chem. Soc.* **2004**, *126*, 15636−15637.

(18) (a) Hecht, S.; Fréchet, J. M. J. *Angew. Chem., Int. Ed. Engl.* **2001**, *40*, 74−91. (b) Cardona, C. M.; Mendoza, S.; Kaifer, A. E. *Chem. Soc. Rev.* **2000**, *29*, 37−42. (c) Gorman, C. B. *C.R. Chimie* **2003**, *6*, 911−918.

(19) (a) Stefanick, J. F.; Ashley, J. D.; Kiziltepe, T.; Bilgicer, B. *ACS Nano* **2013**, *7*, 2935−2947. (b) Knop, K.; Hoogenboom, R.; Fisher, D.; Schubert, U. *Angew. Chem., Int. Ed.* **2010**, *49*, 6288−6308.

(20) (a) Leppiniemi, J.; Määttä, J. A. E.; Hammaren, H.; Soikkeli, M.; Laitaoja, M.; Jänis, J.; Kulomaa, M. S.; Hytönen, V. P. *PLoS One* **2011**, *6*, e16576. (b) Livnah, O.; Bayer, E. A.; Wilchek, M.; Sussman, J. L. *Proc. Natl. Acad. Sci. U.S.A.* **1993**, *90*, 5076−5080. (c) Le Droumaguet, B.; Nicolas, J.; Brambilla, D.; Mura, S.; Maksimenko, A.; De Kimpe, L.; Salvati, E.; Zona, C.; Airoldi, C.; Canovi, M.; Gobbi, M.; Noiray, M.; La Ferla, B.; Nicotra, F.; Scheper, W.; Flores, O.; Masserini, M.; Andrieux, K.; Couvreur, P. *ACS Nano* **2012**, *6*, 5866−5879.

(21) (a) Nantalaksakul, A.; Dasari, R. R.; Ahn, T.-S.; Al-Kaysi, R.; Bardeen, C. J.; Thayumanavan, S. *Org. Lett.* **2006**, *8*, 2981−2984. (b) Dichtel, W. R.; Hecht, S.; Fréchet, J. M. J. *Org. Lett.* **2005**, *7*, 4451−4454. (c) Ornelas, C.; Pennell, R.; Liebes, L. F.; Weck, M. *Org. Lett.* **2011**, *13*, 976−979.

(22) (a) Kolb, H. C.; Finn, M. G.; Sharpless, K. B. *Angew. Chem., Int. Ed.* **2001**, *40*, 2005−2021. (b) Bock, V. D.; Hiemstra, H.; van Maarseveen, J. H. *Eur. J. Org. Chem.* **2006**, *2006*, 51−68. (c) Carlmark, A.; Hawker, C.; Hult, A.; Malkoch, M. *Chem. Soc. Rev.* **2009**, *38*, 352−

362. (d) Helms, B.; Mynar, J. L.; Hawker, C. J.; Fréchet, J. M. J. *J. Am. Chem. Soc.* **2004**, *126*, 15020−15021.
(23) (a) Ryu, J-H; Bickerton, S.; Zhuang, J.; Thayumanavan, S. *Biomacromolecules* **2012**, *13*, 1515−1522. (b) Ryu, J.-H.; Chacko, R. T.; Jiwpanich, S.; Bickerton, S.; Babu, R. P.; Thayumanavan, S. *J. Am. Chem. Soc.* **2010**, *132*, 17227−17235.
(24) (a) Ranganathan, R.; Vautier-Giongo, C.; Bales, B. L. *J. Phys. Chem. B* **2003**, *107*, 10312−10318. (b) Lakowicz, J. R. *Principles of Fluorescence Spectroscopy*, 3rd ed.; Springer: Baltimore, MD, 2006.
(25) (a) Pavan, G. M.; Barducci, A.; Albertazzi, L.; Parrinello, M. *Soft Matter* **2013**, *9*, 2593−2597. (b) Albertazzi, L.; Brondi, M.; Pavan, G. M.; Sulis Sato, S.; Signore, G.; Storti, B.; Ratto, G. M.; Beltram, F. *PLoS ONE* **2011**, *6*, e28450.
(26) Case, D. A.; Darden, T. A.; Cheatham, T. E., III; Simmerling, C. L.; Wang, J.; Duke, R. E.; Luo, R.; Walker, R. C.; Zhang, W.; Merz, K. M.; Roberts, B.; Hayik, S.; Roitberg, A.; Seabra, G.; Swails, J.; Goetz, A. W.; Kolossvary, I.; Wong, K. F.; Paesani, F.; Vanicek, J.; Wolf, R. M.; Liu, J.; Wu, X.; Brozell, S.; Steinbrecher, T.; Gohlke, H.; Cai, Q.; Ye, X.; Wang, J.; Hsieh, M.-J.; Cui, G.; Roe, D. R.; Mathews, D. H.; Seetin, M. G.; Salomon-Ferrer, R.; Sangui, C.; Babin, V.; Luchko, T.; Gusarov, S.; Kovalenko, A.; Kollman, P. A. *AMBER 12*; University of California: San Francisco, CA, 2012.
(27) (a) Doni, G.; Kostiainen, M. A.; Danani, A.; Pavan, G. M. *Nano Lett.* **2011**, *11*, 723−728. (b) Garzoni, M.; Okuro, K.; Ishii, N.; Aida, T.; Pavan, G. M. *ACS Nano* **2014**, *8*, 904−914. (c) Kostiainen, M. A.; Kotimaa, J.; Laukkanen, M.-L.; Pavan, G. M. *Chem.—Eur. J.* **2010**, *16*, 6912−6918.
(28) Klaikherd, A.; Sandanaraj, B. S.; Vutukuri, D. R.; Thayumanavan, S. *J. Am. Chem. Soc.* **2006**, *128*, 9231−9237.
(29) (a) Green, N. M. *Adv. Protein Chem.* **1975**, *29*, 85−133. (b) General, I. J.; Dragomirova, R.; Meirovitch, H. *J. Phys. Chem. B* **2012**, *116*, 6628−6636. (c) Chandler, D. *Introduction to Modern Statistical Mechanics*, 3rd ed.; Oxford University Press: New York, NY, 1987.
(30) Kollman, P. A.; Massova, I.; Reyes, C.; Kuhn, B.; Huo, S. H.; Chong, L.; Lee, M.; Lee, T.; Duan, Y.; Wang, W.; Donini, O.; Cieplak, P.; Srinivasan, J.; Case, D. A.; Cheathaman, T. E. *Acc. Chem. Res.* **2000**, *33*, 889−897.
(31) Kasimova, A. O.; Pavan, G. M.; Danani, A.; Mondon, K.; Cristiani, A.; Scapozza, L.; Gurny, R.; Möller, M. *J. Phys. Chem. B* **2012**, *116*, 4338−4345.
(32) (a) Pavan, G. M.; Danani, A.; Pricl, S.; Smith, D. K. *J. Am. Chem. Soc.* **2009**, *131*, 9686−9694. (b) Munoz, E. M.; Correa, J.; Fernandez-Megia, E.; Rigueira, R. *J. Am. Chem. Soc.* **2009**, *131*, 17765−17767.
(33) (a) Tomalia, D. A.; Uppuluri, S.; Swanson, D. R.; Li, J. *Pure Appl. Chem.* **2000**, *12*, 2343−2358. (b) Tomalia, D. A. *Soft Matter* **2010**, *6*, 456−474.
(34) Khelashvili, G.; LeVine, M. V.; Shi, L.; Quick, M.; Javitch, J. A.; Weinstein, H. *J. Am. Chem. Soc.* **2013**, *135*, 14266−14275.
(35) Ramireddy, R. R.; Subrahmanyam, A. V.; Thayumanavan, S. *Chem.—Eur. J.* **2013**, *19*, 16374−16381.